

# Lattice-Code Multiple Access: Architecture and Efficient Algorithms

Tao Yang, *Member, IEEE*, Fangtao Yu, Rongke Liu, *Senior Member, IEEE*, Shanxiang Lyu, *Member, IEEE* and John Thompson, *Fellow, IEEE*

**Abstract**—This paper studies a  $K$ -user lattice-code based multiple-access (LCMA) scheme. Each user equipment (UE) encodes its message with a practical lattice code, where we suggest a  $2^m$ -ary ring code with symbol-wise bijective mapping to  $2^m$ -PAM. The coded-modulated signal is spread with its designated signature sequence, and all  $K$  UEs transmit simultaneously. The LCMA receiver chooses some integer coefficients, computes the associated  $K$  streams of integer linear combinations (ILCs) of the UEs' messages, and then reconstructs all UEs' messages from these ILC streams. To execute this, we put forth new efficient LCMA soft detection algorithms, which calculate the a posteriori probability of the ILC over the lattice. The complexity is of order no greater than  $O(K)$ , suitable for massive access of a large  $K$ . The soft detection outputs are forwarded to  $K$  ring-code decoders, which employ  $2^m$ -ary belief propagation to recover the ILC streams.

To identify the optimal integer coefficients of the ILCs, a new “bounded independent vectors problem” (BIVP) is established. We then solve this BIVP by developing a new rate-constraint sphere decoding algorithm, significantly outperforming existing LLL and HKZ lattice reduction methods. Then, we develop optimized signature sequences of LCMA using a new target-switching steepest descent algorithm. With our developed algorithms, LCMA is shown to support a significantly higher load of UEs and exhibits dramatically improved error rate performance over state-of-the-art multiple access schemes such as interleave-division multiple-access (IDMA) and sparse-code multiple-access (SCMA). The advances are achieved with just parallel processing and  $K$  single-user decoding operations, avoiding the implementation issues of successive interference cancellation and iterative detection.

**Index Terms**—Multiple access, MIMO, coded modulation, lattice-codes, lattice reduction, compute-forward, physical-layer network coding, iterative detection, soft detection

## I. INTRODUCTION

The multiple access (MA) problem is about how to support reliable communication of  $K$  user equipments (UEs) within  $N$  resource blocks in time, frequency and spatial domains. For very large values of  $K$ , it becomes a massive access problem that is essential to “ubiquitous massive connectivity” envisaged for 6G [1]. It is well-known that orthogonal MA is fundamentally limited from the following perspective. First, the number of supported UEs  $K$  is capped by the number of resource blocks  $N$ . Second, dynamic resource allocation is required to maintain the orthogonality, where the signaling cost could skyrocket as  $K$  becomes large. Third, despite the orthogonalization at the transmitters, the wireless channel induces signal distortion that can easily destroy the orthogonality [2], [3]. Thus, orthogonal MA may not be a suitable choice for massive access.

This work is supported by the National Natural Science Foundation (No. 62371020), Natural Science Foundation of Beijing (No. L232044) and National Key R&D Program of China (No.2020YFB1807102 and No. 2022YFB2902604). This work was partly presented in IEEE Globecom 2023.

Non-orthogonal MA (NoMA) allows collisions of multiple UEs' packets. As such, the number of UEs  $K$  can go beyond the number of resource blocks  $N$  [4]. Further, one can trade-in a higher  $K$  by reducing the peak rates of individual UEs, providing a high flexibility that are very much desired for ubiquitous MA [1]. Moreover, NoMA enables grant-free (GF) transmission, with which the signalling overhead incurred by dynamic resource allocation can be slashed, making it possible to realize massive access in 6G.

### A. Motivations

The core issue of MA is how to deal with multi-UE interference (MUI). Most existing NoMA schemes are based on interference suppression and cancellation, as in power-domain NoMA with successive interference cancellation (SIC) and code-domain NoMA with iterative detection and decoding (IDD) [5]. In theory, such mechanism generally leads to a reduced system load ( $K/N$ ). In practice, SIC and IDD are subject to issues such as rate loss, error propagation, slow and unguaranteed convergence, which have prevented them from being implemented in 5G. This motivates us to study efficient MA approaches that can avoid the issues SIC and IDD in existing NoMA.

### B. Contributions

In this paper, we suggest a lattice-code based MA (LCMA) system. In contrast to conventional NoMA schemes that suppress and cancel MUI, LCMA embraces MUI by exploiting the mapping between the structure of  $K$  UEs' superimposed signal and the lattice space. In the uplink,  $K$  user equipments (UEs) encode their messages with a  $2^m$ -ary ring code, which are then bijectively mapped to  $2^m$ -PAM symbol-by-symbol. Such coded-modulation belongs to the ensemble of lattice codes with easy implementation. Each UE's coded-modulated signal is spread with its designated signature sequence, specifically designed for LCMA, and all UEs transmit simultaneously. The LCMA receiver chooses some integer coefficients, computes the associated  $K$  streams of integer linear combinations (ILCs) of the UEs' messages, and then reconstructs all UEs' messages from these ILC streams. This paper contributes to this subject by developing a package of efficient algorithms involving:

- 1) Simple yet powerful lattice codes that are in line with the mainstream  $2^m$ -QAM modulation.
- 2) Efficient LCMA soft detection algorithms whose per-UE complexity is less than  $O(K)$ .
- 3) A new rate-constrained sphere-decoding algorithm that identifies the optimized LCMA integer coefficients.
- 4) A new target-switching steepest descent algorithm for the optimized LCMA signature sequences.

We demonstrate that the developed LCMA system exhibits much higher MA system loads  $K/N$  and lower error rates over baseline NoMA schemes such as interleave-division MA (IDMA) and sparse-code MA (SCMA). For example, LCMA achieves system loads of up to  $K/N = 350\%$  in Gaussian MA channel and multi-user MIMO channel, which dramatically outperforms IDMA and SCMA that can barely achieve  $K/N = 200\%$ . Meanwhile, ultra-low block error rate (BLER) of  $10^{-6}$  to  $10^{-7}$  is demonstrated for LCMA, which is rarely seen in conventional MA schemes. Such advanced MA functionality and performance are achieved with low-latency parallel processing, low detection complexity of order less than  $O(K)$  per-user, and exactly  $K$  channel-code decoding operations, without the need of SIC or IDD. Also, off-the-shelf channel codes such as 5G NR LDPC codes can be directly used in LCMA for any system load, avoiding the issue of adaptation of channel-code and multi-user detector in IDMA.

### C. Related Literature

1) *Multiple-access*: MA schemes based on interference cancellation and suppression have been studied in the past two decades [3], [6]. Not long after the discovery of turbo codes in 1993, the “turbo principle” was introduced for the multi-user decoding, first by Wang & Poor [7]. Since 2000, turbo-like IDD has been extensively researched. In “turbo-CDMA” [7], the inner code is a multi-user detector with soft interference cancellation and linear minimum MSE (MMSE) suppression, while the outer code is a bank of  $K$  convolutional code decoders. Soft probabilities are exchanged among these components iteratively. In 2006, Li *et al.* introduced a chip-level interleaved CDMA, named interleave-division multiple-access (IDMA) [8]. The chip interleaver enables uncorrelated chip interference, and thus a simple matched filter optimally combines the chip-level signal to yield the symbol-level soft information.

Low-density spreading CDMA and sparse-code MA (SCMA) differ from IDMA in that each symbol-level signal is spread only to a small number of chips, which forms a sparse matrix in the representation of the multi-user signal that can be depicted using a bi-partite factor graph [9]. SCMA also supports grant-free (GF) MA mode for the massive-connectivity scenario. Spatially coupled codes were also studied for dealing with the MA problem, yielding enlarged admissible region for fading MA channels [10]. For IDMA and SCMA, spreading/sparse codes with irregular degree profiles were investigated including the work of ourselves [9], [11], which yielded improved convergence behavior of the multi-user decoding.

Rate-splitting MA (RSMA) was studied for closed-loop systems [12], [13]. The idea is to superimpose a common message on the private messages, which may enlarge the rate-region. Other code-domain NoMA techniques are proposed such as pattern division MA (PDMA), multi-user shared access (MUSA) etc. [14], which exhibits some advantages for implementation. For grant-free MA, active user identification based on compressive sensing and coded slotted Aloha protocols are studied [15]–[17], which significantly reduces the signaling overhead that is essential to massive access. Here we are not able to list all existing results in the area of MA, and readers are encouraged to refer to the excellent survey in [2]. Note that most

existing MA schemes rely on the notion of “rejecting MUI”, where the MUI structure is not or insufficiently exploited.

2) *Literature of Lattice-codes*: For general multi-user networks, it has been proved that “structured codes” based on lattices can achieve a larger capacity region compared to conventional “random-like coding”. The proof was based on the idea of “algebraic binning” of codewords, where each bin collects a certain subset of all codewords. The structure of lattice-codes enables efficient generation of the bin-indices as in the source coding with side information (SI) problem, and efficient decoding of the bin-indices as in the channel coding with SI problem [18]. For physical-layer network coding (PNC) or compute-forward (CF), by adopting lattice-codes at source nodes, the receiver can directly compute the bin-indices in the form of *integer-combinations* of all users’ messages [19], leading to significant coding gain or even multiplexing gain [20], [21]. The work [22] studied simultaneous computation of more than one integer-combinations. The results on using lattice-codes for tackling MIMO detection and downlink MIMO precoding problems were reported in [23] and [24] under the name of integer-forcing (IF). The latter borrowed the notion of reverse CF which exploited the uplink-downlink duality [25], [26]. Various lattice reductions methods for identifying a “good” coefficient matrix for the integer-combinations have been reported in many works such as [27]. Recently, CF and IF have been extended to time-varying or frequency-selective fading channels using multi-mode IF and ring CF [28], [29]. The IF notion was also applied to solve the inter-symbol-interference equalization problem with the help of cyclic linear codes [30]. Here we are not able to list all existing results on lattice-codes, CF and IF, and highly motivated readers are encouraged to refer to [18] and [22].

3) *Lattice-codes and MA*: From an information theoretic perspective, Zhu and Gastpar showed that any rate-tuple of the entire Gaussian MA capacity region can be achieved using a lattice-code based approach, and the scheme was named compute-forward MA (CFMA) [31]. In contrast to random-like coding approaches exploited in existing NoMA schemes, lattice-code based MA exhibits a greater capacity region, which is achieved with low-cost single-user decoding. The design of CFMA for the Gaussian MA channel with binary codes was studied in [32]. Recently, we extend the result of [31] and [32] to fading MA channel with practical  $q$ -ary codes [33], [34]. To date, most of the related works on lattice-codes for MA have been focusing on achievable rates by proving the existence of “good” nested lattice-codes, whereas the practical aspects are not yet sufficiently researched. The methods developed in [32] and [34] do not apply to practical  $2^{2^m}$ -QAM signaling and MIMO. The impacts of lattice-codes on the key performance indicators such as the system load, BLER, latency, complexity and etc., are still to be investigated. In addition, for a large  $K$ , there lacks efficient algorithms for both the soft detection and the identification of the coefficient matrix with realistic implementation costs. This motivates us to develop a package of practical coding, efficient signal processing algorithms and optimization methods for lattice-code MA in this paper.

## II. SYSTEM MODEL

Consider an uplink MA system where  $K$  single-antenna UEs deliver messages to a common base station (BS). Let a row vector  $\mathbf{x}_i^T$  denote the transmitted coded symbol sequence of UE  $i$ ,  $i = 1, \dots, K$ , with a normalized average energy per-symbol.

### A. Scenario I. Gaussian Multiple Access

For a Gaussian MA channel (G-MAC), the received signal at the single-antenna BS is given by a row vector

$$\mathbf{y}^T = \sum_{i=1}^K \sqrt{\rho_i} \mathbf{x}_i^T + \mathbf{z}^T \quad (1)$$

where  $\mathbf{z}^T$  denotes the additive white Gaussian noise (AWGN) sequence whose entries are i.i.d. with mean 0 and variance  $\sigma_z^2 = 1$ . The average per-UE signal-to-noise ratio (SNR) is given by  $\rho$ ,

where  $\rho = \frac{1}{K} \sum_{i=1}^K \rho_i$ . The G-MAC model has high interests from a theoretical point of view. Also, such model applies to line-of-sight dominant practical systems, e.g. a satellite communication where a single-beam is allocated for a certain geographical area containing a large number of UEs<sup>1</sup>.

### B. Scenario II. Multi-UE (MU) MIMO

For a (narrow-band) MU-MIMO channel, the baseband equivalent discrete signal received at the  $N_R$ -antenna BS can be presented by the following real-valued model

$$\mathbf{Y} = \sum_{i=1}^K \mathbf{h}_i \sqrt{\rho} \mathbf{x}_i^T + \mathbf{Z} = \sqrt{\rho} \mathbf{H} \mathbf{X} + \mathbf{Z} \quad (2)$$

where the column vector  $\mathbf{h}_i$  denotes the channel coefficients from UE  $i$  to the  $N_R$  antennas of the BS; the  $j$ th row of  $\mathbf{Y}$  denotes the signal sequence received by antenna  $j$ ,  $j = 1, \dots, N_R$ ;  $\mathbf{Z}$  denotes the AWGN matrix. For the ease of presentation, identical power among UEs is utilized in (2), while our treatment is also applicable to unequal power allocation.

A complex-valued model can be represented by a real-valued model of doubled dimension of  $2N_R$ -by- $2K$ , i.e.,

$$\begin{bmatrix} \mathbf{Y}^{\text{Re}} \\ \mathbf{Y}^{\text{Im}} \end{bmatrix} = \sqrt{\rho} \begin{bmatrix} \mathbf{H}^{\text{Re}} & -\mathbf{H}^{\text{Im}} \\ \mathbf{H}^{\text{Im}} & \mathbf{H}^{\text{Re}} \end{bmatrix} \begin{bmatrix} \mathbf{X}^{\text{Re}} \\ \mathbf{X}^{\text{Im}} \end{bmatrix} + \begin{bmatrix} \mathbf{Z}^{\text{Re}} \\ \mathbf{Z}^{\text{Im}} \end{bmatrix} \quad (3)$$

following [19], [35]. This paper presents with real-valued model for the clarity of notation and better readability.

This paper is primarily interested in studying the configuration of  $K \geq N_R$ . In particular, for  $K$  being very large, the scenario is referred to “*massive access MIMO*”. Such configuration is different from conventional *massive MIMO* in the literature, where  $N_R$  is very large while the number of UE is far less, i.e.  $K \ll N_R$ . Note that a fading MAC model, where each user’s signal undergoes a channel gain and phase rotation, is equivalent to the MU-MIMO setup with  $N_R = 1$ . Such fading MAC model is sitting in between the Gaussian MAC and MU-MIMO models described above.

<sup>1</sup>In this paper we assume that the signals of the UEs are synchronized at the receiver. This is done in the initial access stage prior to the data transmission stage considered in this paper.

### C. Performance Indicators

Following the convention in studying the uplink MA, we consider an open-loop system where there is no feedback to the UE transmitters to deliver the channel state information (CSI) and implement adaptive coding and modulation (ACM). Each UE transmits at a target *per-user data rate*  $R_0$ . The key performance indicators of the MA system are the *supported system load* given by  $K/N$ , and *block error rate* (BLER).

The problem under consideration is: how to design a MA transceiver architecture and processing algorithms, such that the MA system supports a high system load while meeting a target BLER, or achieves a low BLER for a given system load.

## III. ARCHITECTURE OF LATTICE-CODE MULTIPLE ACCESS

The architecture of a LCMA system is depicted in Fig. 1. Our treatment applies to both G-MAC and MU-MIMO (as will be specified in Section IV. F).

### A. LCMA Transmitters

#### 1) Encoding and Modulation with a Practical Lattice-code:

Let  $\mathbf{b}_i = [b_i[1], \dots, b_i[k]]^T$  denote the message sequence of UE  $i$ ,  $i = 1, \dots, K$ . Each entry of  $\mathbf{b}_i$  belongs to an integer ring<sup>2</sup>  $\mathbb{Z}_{2^m} \triangleq \{0, \dots, 2^m - 1\}$ ,  $m = 1, 2, \dots$ . For a general value of  $m$ , we suggest to utilize a  $2^m$ -ary ring code, with *generator matrix*  $\mathbf{G}$  of size  $n$ -by- $k$ , to encode the message sequences of the  $K$  UEs. The resultant coded sequences are given by

$$\mathbf{c}_i = \text{mod}(\mathbf{G}\mathbf{b}_i, 2^m) = \mathbf{G} \otimes \mathbf{b}_i, i = 1, \dots, K, \quad (4)$$

where “ $\otimes$ ” represents matrix multiplication modulo- $2^m$ .

The entries of each UE’s coded sequence  $\mathbf{c}_i = [c_i[1], \dots, c_i[n]]^T$  are mapped *one-to-one* to symbols in a  $2^m$ -PAM constellation, given by

$$x_i[t] = \frac{1}{\gamma} \left( c_i[t] - \frac{2^m - 1}{2} \right) \in \frac{1}{\gamma} \left\{ \frac{1 - 2^m}{2}, \dots, \frac{2^m - 1}{2} \right\}. \quad (5)$$

Here  $\gamma$  normalizes the average symbol energy.

The above  $2^m$ -ary ring-coded PAM executed via (4) and (5) is a lattice code, which utilizes a simple one-dimension shaping lattice [36] [18] [20]. Such a lattice code matches with the mainstream  $2^{2^m}$ -QAM signaling<sup>3</sup>. The per-user rate of such a lattice code is  $R_0 = \frac{k}{n} \log_2 2^m = \frac{km}{n}$  bits/symbol<sup>4</sup>. For  $m = 1$ , any existing binary code (such as LDPC or polar codes in the 5G standard) applies, where  $\mathbf{c}_i$  is a binary sequence while  $\mathbf{x}_i = [x_i[1], \dots, x_i[n]]$  is a BPSK symbol sequence. For a general  $m$ , LPDC codes and capacity approaching doubly irregular accumulate codes over  $2^m$ -ary rings that we developed previously can be utilized [37].

<sup>2</sup>The conversion from a binary message sequence to a  $2^m$ -ary message sequence is straightforward. Our development applies to a  $q$ -ary code with  $q$ -PAM for any  $q$ , either prime or non-prime, while this paper only presents with non-prime  $q = 2^m$ .

<sup>3</sup>For a complex-valued model, two independent  $2^m$ -level ring-coded PAM, one for the in-phase and the other for the quadrature part, form a lattice code with  $2^{2^m}$ -QAM signaling. For a better readability, this paper presents with the real-valued model.

<sup>4</sup>The extension to the asymmetric rate setup is straightforward. A low rate UE’s message is zero-padded to form a length  $k$  message sequence. Then, the same channel code encoder is utilized to encode all UEs’ messages.

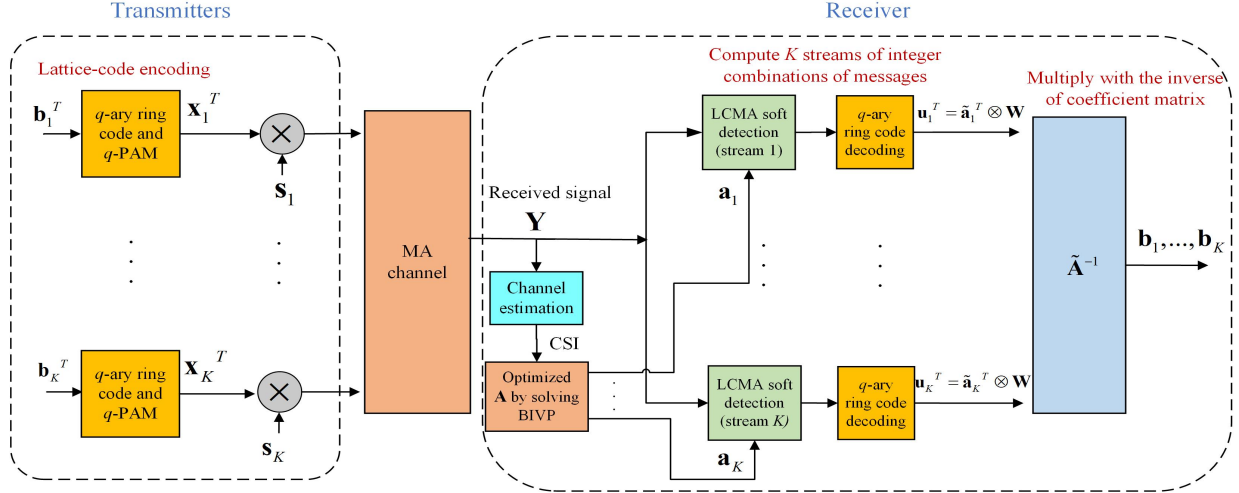


Fig. 1. Block diagram of the transmitters and receiver of a LCMA system. All users utilize the same  $2^m$ -ary RCM. No interleavers and deinterleavers are used. For each MA channel realization, the optimized coefficient matrix  $\mathbf{A}$  is identified by solving the BIVP w.r.t. the channel state information. The LCMA soft detection and decoding of the  $K$  streams are implemented in parallel.

2) *Spreading for MA*: We suggest to multiply the *symbol-level* signal  $x_i[t]$  of UE  $i$  with its designated spreading signature sequence  $\mathbf{s}_i$  of length  $N_S$ , yielding the *chip-level* signal  $\mathbf{s}_i x_i[t]$ . The chip-level signal sequence can be written as

$$[\mathbf{s}_i^T x_i[1], \dots, \mathbf{s}_i^T x_i[n]], i = 1, \dots, K. \quad (6)$$

Then all  $K$  UEs transmit simultaneously.

The spreading sequences satisfy a total power constraint

$$\sum_{i=1}^K \|\mathbf{s}_i\|^2 \leq K. \quad (7)$$

Compared to other existing MA schemes, the distinguishing features of LCMA transmitter involve: a lattice code formed via  $2^m$ -ary ring code coupled with a one-to-one  $2^m$ -PAM mapping<sup>5</sup>, a spreading matrix  $\mathbf{S} = [\mathbf{s}_1, \dots, \mathbf{s}_K]$  whose design is coupled with the LCMA receiver's processing (to be presented next), and the removal of the symbol-level or chip-level interleavers [7] [38]. Note that even for  $m = 1$ , lattice-based processing and design are required.

### B. LCMA Receiver

The received signal at the BS is given by<sup>6</sup>

$$\mathbf{Y} = \sum_{i=1}^K \mathbf{s}_i^T \mathbf{x}_i + \mathbf{Z}. \quad (8)$$

The  $j$ th row stands for the signal w.r.t. the  $j$ th chip,  $j = 1, \dots, N_S$ . The task of the BS receiver is to recover all  $K$  UE's message sequences  $\mathbf{b}_1, \dots, \mathbf{b}_K$ .

The receiver architecture is shown in Fig. 1. The notion of the LCMA's receiver processing is to efficiently compute  $K$  independent streams of *integer linear combinations* (ILCs) of the UE' messages, with the help of the structural property of the underlying lattice code.

<sup>5</sup>This differs from conventional bit-interleaved coded modulation, trellis coded modulation and multi-level coding schemes.

<sup>6</sup>For clarity, this paper presents with receiver-side synchronization setup. The developed LCMA also applies to the setup with asynchrony among the UEs.

*Definition 1*: The  $l$ th stream of *message-level* ILC is defined as

$$\mathbf{u}_l^T \triangleq \text{mod} \left( \sum_{i=1}^K a_{l,i} \mathbf{b}_i^T, 2^m \right) = \mathbf{a}_l^T \otimes \mathbf{B}, l = 1, \dots, K, \quad (9)$$

where  $\mathbf{B} = [\mathbf{b}_1, \dots, \mathbf{b}_K]^T$ ,  $\mathbf{a}_l = [a_{l,1}, \dots, a_{l,K}]^T$  denotes the associated *integer coefficient vector*.

Let  $\mathbf{U} = [\mathbf{u}_1, \dots, \mathbf{u}_K]^T$  consist of all  $K$  streams of ILC. Let  $\mathbf{A} = [\mathbf{a}_1, \dots, \mathbf{a}_K]^T$  stack up all  $K$  coefficient vectors, referred to as the ILC *coefficient matrix*. Denote  $\mathbf{A}$  modulo- $2^m$  by  $\tilde{\mathbf{A}} = \text{mod}(\mathbf{A}, 2^m)$ , then

$$\mathbf{U} = \tilde{\mathbf{A}} \otimes \mathbf{B}. \quad (10)$$

In LCMA, it is required that  $\tilde{\mathbf{A}}$  is of full rank  $K$  in  $\mathbb{Z}_{2^m}$ , thus it has a unique inverse  $\tilde{\mathbf{A}}^{-1}$ , i.e.,  $\tilde{\mathbf{A}}^{-1} \otimes \tilde{\mathbf{A}} = \mathbf{I}$ . If all streams of ILCs  $\mathbf{u}_1, \dots, \mathbf{u}_K$  are correctly computed, all  $K$  users' messages can be recovered by implementing

$$\mathbf{B} = \tilde{\mathbf{A}}^{-1} \otimes \mathbf{U}. \quad (11)$$

*Remark 1*: Conventionally, the BS receiver performs UE-by-UE detection and decoding w.r.t.  $\mathbf{b}_1, \dots, \mathbf{b}_K$ . The LCMA receiver goes beyond this. It first performs ILC-by-ILC detection and decoding w.r.t.  $\mathbf{u}_1, \dots, \mathbf{u}_K$ , and then retrieves the message sequences via (11). LCMA has the room to identify the best matrix  $\mathbf{A}$  that leads to the most efficient ILC-by-ILC processing, which translates into enhanced system load or error rate performance. When  $\mathbf{A}$  is set to  $\mathbf{I}$ , LCMA receiver reduces to conventional UE-by-UE processing. Note that the computation of the  $K$  integer combinations are performed in parallel, where only the  $l$ -th row of  $\mathbf{A}$  is needed in computing the  $l$ -th integer linear combination.

### C. LCMA Design Problems to be Addressed

For the LCMA receiver, the design problems involve:

- Efficient computation of  $K$  ILC streams  $\mathbf{U} = [\mathbf{u}_1, \dots, \mathbf{u}_K]^T$  by exploiting the structural property of the

underlying lattice code. Practical algorithms for this will be developed in Section IV.

- Identification of the optimal ILC coefficient matrix  $\mathbf{A}$ . This will be studied in Section V.A.

For the LCMA transmitters, the design problem is:

- Optimized design of the MA signature matrix  $\mathbf{S}$ . This problem is coupled with the receiver processing, and will be studied in Section V.B.

#### IV. ALGORITHMS OF SOFT LCMA DETECTION AND DECODING

This section is devoted to the efficient computation of the ILC streams  $\mathbf{U} = [\mathbf{u}_1, \dots, \mathbf{u}_K]^T$ , where  $\mathbf{A}$  is given. We focus on a *parallel rule*<sup>7</sup> for computing the a posteriori probabilities (APPs) of the  $K$  ILC streams, given by

$$p(\mathbf{u}_l | \mathbf{Y}), l = 1, \dots, K. \quad (12)$$

The execution of (12) relies on a crucial property of the underlying lattice code presented below.

##### A. Property of Lattice code Exploited in LCMA

Recall the coded sequences  $\mathbf{c}_i$  generated in (4). Let  $\mathbf{C} = [\mathbf{c}_1, \dots, \mathbf{c}_K]^T$ .

*Definition 2:* The  $l$ th stream of *codeword-level* ILC is defined as

$$\mathbf{v}_l^T \triangleq \text{mod} \left( \sum_{i=1}^K a_{l,i} \mathbf{c}_i^T, 2^m \right) = \mathbf{a}_l^T \otimes \mathbf{C}, l = 1, \dots, K. \quad (13)$$

*Property 1:* With the  $2^m$ -ary ring code utilized in (4), we have

$$\mathbf{v}_l = \mathbf{G} \otimes \text{mod} \left( \sum_{i=1}^K a_{l,i} \mathbf{b}_i, 2^m \right) = \mathbf{G} \otimes \mathbf{u}_l. \quad (14)$$

For point-to-point communication, the codeword  $\mathbf{c}$  and the message sequence  $\mathbf{b}$  are related by the generator matrix  $\mathbf{G}$  as in (4). For the  $K$ -user MA setting under consideration, Property 1 indicates that the codeword-level ILC  $\mathbf{v}_l$  and the message-level ILC  $\mathbf{u}_l$  are also related by the generator matrix  $\mathbf{G}$  as in (14). (This property does not apply to conventional non-lattice code based schemes such as bit-interleaved coded modulation (BICM), trellis coded modulation (TCM) and superposition coded modulation (SCM).)

Thanks to Property 1, a “two-step” method applies:

Step 1) **Soft ILC Detection**: computes  $p(\mathbf{v}_l | \mathbf{Y})$ , i.e., the APPs of the codeword-level ILC  $\mathbf{v}_l$ .

Step 2) **Ring-code Decoding**: takes in  $p(\mathbf{v}_l | \mathbf{Y})$  as input for decoding, which outputs a decision on the message-level ILC  $\mathbf{u}_l$ .

<sup>7</sup>The parallel rule can be enhanced by a successive rule [34]. This paper focus on the parallel rule owing to its low-cost implementation, tractable analysis and optimization. Later we will see that the parallel rule yields competitive performance.

##### B. LCMA Soft ILC Detection

Here we consider Step 1) for the  $l$ -th ILC stream. The soft ILC detection calculates

$$p(v_l[t] | \mathbf{y}[t]), t = 1, \dots, n \quad (15)$$

in a symbol-wise manner.

This paper focuses on a linear LCMA soft detector to calculate (15). (The non-linear LCMA detector is studied in a separate work [39].) The notion is to first transform the  $N_S$ -dimension received signal into  $K$  streams of single-dimension signals. Then, each stream is used to compute one ILC.

Let a length- $N_S$  vector  $\mathbf{w}_l$  denote the linear filter w.r.t the  $l$ th ILC stream, which is normalized to  $\|\mathbf{w}_l\| = 1$ . For symbol-by-symbol detection, we can omit the symbol index “ $t$ ” below. The  $l$ th filtered signal stream is

$$\tilde{y}_l = \mathbf{w}_l^T \mathbf{y} = \mathbf{w}_l^T \sum_{i=1}^K \sqrt{\rho} \mathbf{s}_i x_i + \tilde{z}_l \quad (16)$$

$$= \sum_{i=1}^K \sqrt{\rho} \psi_{l,i} x_i + \tilde{z}_l. \quad (17)$$

where  $\psi_{l,i} = \mathbf{w}_l^T \mathbf{s}_i$  denotes the “effective gain” w.r.t. UE  $i$ 's signal, and the noise term  $\tilde{z}_l$  has a unit variance. Our developed soft detection algorithm below applies to any  $\mathbf{w}_l$ .

Let the set  $\mathcal{I}_l \triangleq \{i : a_{l,i} \neq 0\}$  collects the positions of non-zero entries of  $\mathbf{a}_l$ , and  $\mathcal{I}_l^c$  be the complementary set. Let  $\omega(\mathbf{a}_l) \triangleq |\mathcal{I}_l|$  denote the number of non-zero entries. Then,  $\tilde{y}_l$  is re-arranged as

$$\tilde{y}_l = \sum_{i \in \mathcal{I}_l} \sqrt{\rho} \psi_{l,i} x_i + \sum_{i \in \mathcal{I}_l^c} \sqrt{\rho} \psi_{l,i} x_i + \tilde{z}_l = \sum_{i \in \mathcal{I}_l} \sqrt{\rho} \psi_{l,i} x_i + \xi_l. \quad (18)$$

The term  $\sum_{i \in \mathcal{I}_l} \sqrt{\rho} \psi_{l,i} x_i$  is the superposition of the signals of the  $\omega(\mathbf{a}_l)$  users whose ILC coefficients are non-zero, which is the *useful signal* part. The term  $\sum_{i \in \mathcal{I}_l^c} \sqrt{\rho} \psi_{l,i} x_i$  contains the signals of the remaining  $K - \omega(\mathbf{a}_l)$  UEs whose ILC coefficients are zero, which can be regarded as irrelevant w.r.t. ILC. The term  $\xi_l = \sum_{i \in \mathcal{I}_l^c} \sqrt{\rho} \psi_{l,i} x_i + \tilde{z}_l$  is treated as the *effective noise*, which is not correlated with the useful signal part.

Recall the one-to-one mapping  $x_i = \frac{1}{\gamma} (c_i - \frac{2^m - 1}{2})$  in (5). For the clarity of presentation, we express the received signal with  $c_i$  (instead of with  $x_i$ ), given as

$$\bar{y}_l = \sum_{i \in \mathcal{I}_l} \sqrt{\rho} \psi_{l,i} \left( \gamma x_i + \frac{2^m - 1}{2} \right) + \gamma \xi_l = \sum_{i \in \mathcal{I}_l} \sqrt{\rho} \psi_{l,i} c_i + \bar{z}_l. \quad (19)$$

For a large  $K$ , it can be shown that  $|\mathcal{I}_l^c|$  is sufficiently large to apply Central Limit Theorem. Then  $\bar{z}_l = \gamma \xi_l$  follows a Gaussian distribution with 0 mean and variance  $\bar{\sigma}_l^2 = \gamma^2 (\rho \sum_{i \in \mathcal{I}_l^c} \psi_{l,i}^2 + 1)$ .

Recall that  $v_l \triangleq \mathbf{a}_l^T \otimes \mathbf{c}$ . With the above arrangement, the APP w.r.t. the  $l$ th ILC is now given by

$$p(v_l = \theta | \bar{y}_l) = \frac{1}{\eta} \sum_{\mathbf{c}: \mathbf{a}_l^T \otimes \mathbf{c} = \theta} \exp \left( - \left| \bar{y}_l - \sum_{i \in \mathcal{I}_l} \sqrt{\rho} \psi_{l,i} c_i \right|^2 / 2\bar{\sigma}_l^2 \right), \quad (20)$$

where  $\eta$  is the normalization factor. The APP  $p(v_l = \theta | \bar{y}_l)$  is equal to the sum of the likelihood functions of the candidates whose underlying ILC is equal to  $\theta$ .

### C. Low-complexity LCMA Soft Detection based on Gaussian Approximation

A direct execution of (20) requires to evaluate the Euclidean distances of  $2^{m\omega(\mathbf{a}_l)}$  candidates of  $\mathbf{c}$ . The order of complexity therein is thus  $O(2^{m\omega(\mathbf{a}_l)})$ . In this part, we develop efficient soft ILC detection algorithms for the computation of (20). The algorithms have per-user complexity (much) less than  $O(K)$ .

In general, there is a many-to-one mapping between  $\mathbf{a}_l^T \mathbf{c}$  and  $\mathbf{a}_l^T \otimes \mathbf{c}$ . Specifically, all the events  $\{\mathbf{a}_l^T \mathbf{c} = \theta \pm \beta \cdot 2^m\}$  with various values  $\bar{\theta} = \theta \pm \beta \cdot 2^m$  have an identical  $\mathbf{a}_l^T \otimes \mathbf{c} = \bar{\theta}$  after the modulo- $2^m$  operation. As such, using the Total Probability Rule, the APP is written as

$$p(v_l = \theta | \bar{y}_l) = \frac{1}{\eta} \sum_{\bar{\theta} : \text{mod}(\bar{\theta}, 2^m) = \theta} p(\bar{y}_l | \mathbf{a}_l^T \mathbf{c} = \bar{\theta}) p(\bar{\theta}). \quad (21)$$

Here we derive the likelihood function  $p(\bar{y}_l | \mathbf{a}_l^T \mathbf{c} = \bar{\theta})$ . Let  $\Omega_l(\bar{\theta}) = \{\mathbf{c} : \mathbf{a}_l^T \mathbf{c} = \bar{\theta}\}$  collect the candidates  $\mathbf{c}$  with  $\mathbf{a}_l^T \mathbf{c}$  equal to  $\bar{\theta}$ . The conditional mean for a given value of  $\mathbf{a}_l^T \mathbf{c} = \bar{\theta}$  is

$$\mu_l(\bar{\theta}) = E_{\mathbf{c}}(\bar{y}_l | \mathbf{a}_l^T \mathbf{c} = \bar{\theta}) = \frac{1}{|\Omega_l(\bar{\theta})|} \sum_{\mathbf{c} \in \Omega_l(\bar{\theta})} \sum_{i \in \mathcal{I}_l} \sqrt{\rho} \psi_{l,i} c_i. \quad (22)$$

The conditional variance is

$$\begin{aligned} \sigma_l^2(\bar{\theta}) &= E_{\mathbf{c}} \left( \left| \sum_{i \in \mathcal{I}_l} \sqrt{\rho} \psi_{l,i} c_i + \bar{z}_l - \mu_l(\bar{\theta}) \right|^2 \right) \\ &= \frac{1}{|\Omega_l(\bar{\theta})|} \sum_{\mathbf{c} \in \Omega_l(\bar{\theta})} \left( \sum_{i \in \mathcal{I}_l} \sqrt{\rho} \psi_{l,i} c_i \right)^2 - \mu_l^2(\bar{\theta}) + \gamma^2 \bar{\sigma}_l^2. \end{aligned} \quad (23)$$

For a sufficiently large  $K$ , the proposed low-complexity algorithm approximates  $\bar{y}_l$  to have a conditional Gaussian distribution for all values of  $\bar{\theta}$ . The APP is then calculated as

$$p(v_l = \theta | \bar{y}_l) = \frac{1}{\eta} \sum_{\bar{\theta} : \text{mod}(\bar{\theta}, 2^m) = \theta} \exp \left( -\frac{(\bar{y}_l - \mu_l(\bar{\theta}))^2}{2\sigma_l^2(\bar{\theta})} \right) p(\bar{\theta}). \quad (24)$$

This is referred to as *Detection Method I* in this paper.

1) *Calculation of the Statistic Values in Detail:* Detection Method I requires a) the a priori probability  $p(\bar{\theta})$ , b) the conditional mean  $\mu_l(\bar{\theta})$  and c) conditional variance  $\sigma_l^2(\bar{\theta})$  (24), to be detailed below. Since these statistics are required to be calculated once per-block, the cost is minor compared to that in (24) which are computed  $n$  times per-block. For notational simplify, the index  $l$  is omitted in this part.

a) Let  $n_1[\bar{\theta}] = 1$  for  $\bar{\theta} = 0, a_1, \dots, (2^m - 1)a_1$  if  $a_1 > 0$ , and  $\bar{\theta} = (2^m - 1)a_1, \dots, 0$  if  $a_1 < 0$ . Let  $n_1[\bar{\theta}] = 0$  for the rest values of  $\bar{\theta}$ . Then  $p(\bar{\theta})$  can be obtained by sequentially implementing

$$n_k[\bar{\theta}] = \sum_{\tau=0, \dots, 2^m-1} n_{k-1}[\bar{\theta} - a_i \tau] \quad (25)$$

until layer  $K' = \omega(\mathbf{a})$  is reached. This requires no more than  $\sum_{k=1}^{K'} (\omega_H([a_1, \dots, a_k]) (2^m - 1) + 1) (2^m - 1) \approx \sum_{k=1}^{K'} \omega_H([a_1, \dots, a_k]) (2^m - 1)^2$  additions in total and does not involve multiplication.

b) The conditional means can be obtained by sequentially implementing

$$\tilde{\mu}_k[\bar{\theta}] = \sum_{\tau=0, \dots, 2^m-1} \tilde{\mu}_{k-1}[\bar{\theta} - a_i \tau] + \tau \sqrt{\rho} \psi_k. \quad (26)$$

When reaching layer  $K' = \omega(\mathbf{a})$ , the conditional mean is computed by  $\mu(\bar{\theta}) = \tilde{\mu}_{K'}[\bar{\theta}] / n_{K'}[\bar{\theta}]$ .

c) The term  $\sum_{\mathbf{c} \in \Omega(\bar{\theta})} \left( \sum_{i \in \mathcal{I}} \sqrt{\rho} \psi_i c_i \right)^2$  is calculated by sequentially implementing  $\vartheta_k[\bar{\theta}] =$

$$\sum_{\tau=0, \dots, 2^m-1} \left( \vartheta_{k-1}[\bar{\theta} - a_k \tau] + 2\tau \sqrt{\rho} \psi_i u_{k-1}[\bar{\theta} - a_k \tau] + (\tau \sqrt{\rho} \psi_i)^2 \right).$$

When reaching layer  $K'$ , the conditional variance is obtained as

$$\sigma^2(\bar{\theta}) = s_{K'}[\bar{\theta}] / n_{K'}[\bar{\theta}] - \mu^2(\bar{\theta}) + \gamma^2 \bar{\sigma}^2. \quad (27)$$

2) *Complexity Analysis:* Here, it can be easily shown that the integer-valued  $\bar{\theta}$  are within the range of

$$\bar{\theta} \in \left\{ \sum_{i: a_{l,i} < 0} a_{l,i} (2^m - 1), \dots, \sum_{i: a_{l,i} > 0} a_{l,i} (2^m - 1) \right\}. \quad (28)$$

Define  $\omega_H(\mathbf{a}_l) \triangleq \sum_{i \in \mathcal{I}_l} |a_{l,i}|$ , referred to as the “weight” of  $\mathbf{a}_l$ .

Then the cardinality of the set for  $\bar{\theta}$  is precisely  $\omega_H(\mathbf{a}_l) (2^m - 1) + 1$ . In other words, there are  $\omega_H(\mathbf{a}_l) (2^m - 1) + 1$  Euclidean distances needs to be calculated in (24). This is far less than  $2^{m\omega(\mathbf{a}_l)}$  required in direct execution of (20).

For all  $K$  ILCs, the total number of Euclidean distance calculations is

$$(2^m - 1) \sum_{l=1}^K \omega_H(\mathbf{a}_l) + K = 2^m K \cdot E_{\mathbf{a}}(\omega_H(\mathbf{a})) \quad (29)$$

where  $E_{\mathbf{a}}(\omega_H(\mathbf{a}))$  is the average weight of coefficient vectors. The average per-user complexity has order  $O(2^m E_{\mathbf{a}}(\omega_H(\mathbf{a})))$ . This is  $E(\omega_H(\mathbf{a}))$  times of the complexity of single-user detection. As we will see later in Section VI,  $E_{\mathbf{a}}(\omega_H(\mathbf{a}))$  is just a fraction of  $K$  in general for  $K$  being large.

### D. Decoding

The soft ILC detection outcome  $p(v_l[t] | \mathbf{y}[t])$ ,  $t = 1, \dots, n$  is forwarded to a ring code decoder, which carried out  $2^m$ -ary decoding algorithm to obtain its soft outputs on the message level ILC  $u_l[t]$ ,  $t = 1, \dots, k$ . For a  $2^m$ -ary LDPC ring code [37], for example,  $2^m$ -ary belief propagation (BP) algorithm is employed. We again note that the soft detection and decoding for the  $K$  ILC streams are executed in parallel. Upon all  $K$  message-level ILCs are calculated, the messages of the  $K$  users are recovered by (11).

### E. Example with Integer-forcing

Our developed algorithm applies to any filter matrix  $\mathbf{W} = [\mathbf{w}_1, \dots, \mathbf{w}_K]^T$ . If exact IF (EIF) is adopted in a  $K \leq N_S$  system, the filter matrix is given by [23]  $\mathbf{W}_{IF} = \mathbf{A} (\mathbf{S}^T \mathbf{S})^{-1} \mathbf{S}^T$ . The signal is then given as

$$\bar{y}_l = \sum_{i \in \mathcal{I}_l} \sqrt{\rho} \psi_{l,i} c_i + \bar{z}_l = \sum_{i \in \mathcal{I}_l} \sqrt{\rho} a_{l,i} c_i + \bar{z}_l. \quad (30)$$

The last equality follows from the fact that  $(\mathbf{S}^T \mathbf{S})^{-1} \mathbf{S}^T \mathbf{S} = \mathbf{I}$ . In this case, the effective gains are exactly identical to the coefficient vectors. Thus,  $\mu_l(\bar{\theta}) = \bar{\theta}$  and  $\sigma_l^2(\bar{\theta}) = \gamma^2 \tilde{\sigma}_l^2$ , which are utilized in (24) to calculate the APP of ILC. The a priori probabilities are required to be calculated as in (25).

The EIF presented above does not support an MA setup of  $K > N_S$ , and suffers from performance loss, particularly at low SNR. Regularized IF (RIF) can address such issues, whose filter matrix is [23]

$$\mathbf{W}_{RIF} = \mathbf{A} \mathbf{S}^T (\rho \mathbf{S} \mathbf{S}^T + \mathbf{I}_N)^{-1}. \quad (31)$$

With  $\mathbf{W}_{RIF}$ , the signal can be written as

$$\bar{y}_l = \sum_{i \in \mathcal{I}_l} \sqrt{\rho} \psi_{l,i} c_i + \bar{z}_l = \sum_{i \in \mathcal{I}_l} \sqrt{\rho} a_{l,i} c_i + e_l. \quad (32)$$

The estimation error term is

$$e_l = \sum_{i \in \mathcal{I}_l} \sqrt{\rho} (\psi_{l,i} - a_{l,i}) c_i + \bar{z}_l. \quad (33)$$

Unlike the EIF, here the error term  $e_l$  in RIF is correlated with the useful signal part  $\sum_{i \in \mathcal{I}_l} \sqrt{\rho} a_{l,i} c_i$ . This leads to  $\mu_l(\bar{\theta}) \neq \bar{\theta}$  and  $\sigma_l^2(\bar{\theta}) \neq \gamma^2 \tilde{\sigma}_l^2$ , which must be calculated as in (22) and (23), respectively.

For a sufficiently large  $K$ , the number of terms that adds up in (33) is sufficiently large to apply Central Limit Theorem for  $e_l$ . Hence, one may approximate  $e_l$  as a Gaussian random variable with variance  $E(e_l^2)$ . It can be easily shown that the MSE of  $e_l$  has a closed-form representation

$$E(e_l^2) = \gamma^2 \mathbf{a}_l^T (\rho \mathbf{S}^T \mathbf{S} + \mathbf{I})^{-1} \mathbf{a}_l^T. \quad (34)$$

Further, by disregarding the bias in the estimation error term, the mean of  $e_l$  is approximated as zero. As such, the calculation of the APP in (24) is further simplified into

$$p(v_l = \theta | \bar{y}_l) \approx \frac{1}{\eta} \sum_{\bar{\theta}: \mathbf{a}_l^T \bar{\mathbf{c}} = \theta} \exp\left(-\frac{(\bar{y}_l - \bar{\theta})^2}{2E(e_l^2)}\right) p(\bar{\theta}). \quad (35)$$

This is referred to as *Detection Method II*, which is inferior to Detection Method I due to the approximation in the conditional mean and variance. Note that the a priori probabilities are required to be calculated as in (25), while the calculations of conditional means and variances are avoided.

For a relatively small number of users  $K$ , Detection Method I is suggested while the loss of Method II may be considerable. For a large value of  $K$ , either Method I or Method II could be used. The receiver processing with linear LCMA detection method II is summarized in Algorithm 1.

---

### Algorithm 1 Summary of LCMA Receiver's Processing (Detection Method II.)

---

Step 1) Calculate the filtering matrix  $\mathbf{W}_{RIF}$  according to (31). Perform the filtering process (32).

Step 2) Calculate the MSE  $E(e_l^2)$  according to (34) for  $l = 1, \dots, K$ . Calculate the a priori probabilities as in (25).

Step 3) Perform (35) in parallel to calculate the APPs  $p(v_l = \theta | \bar{y}_l)$  for the  $K$  streams of codeword-level ILCs. Forward the  $K$  streams of APPs to the  $K$  ring-code decoders.

Step 4) Perform ring-code decoding for the  $K$  streams parallelly, which yields the decisions on  $\mathbf{u}_1, \dots, \mathbf{u}_K$ .

Step 5) Recover  $K$  users' messages by implementing  $\mathbf{B} = \tilde{\mathbf{A}}^{-1} \otimes \mathbf{U}$ .

---

### F. Treatment for MU-MIMO

The LCMA technique and algorithms developed above directly apply to MU-MIMO, by simply replacing the spreading matrix  $\mathbf{S}$  by the MIMO channel coefficient matrix  $\mathbf{H}$  in executing the LCMA receiver processing. A slight difference is that one may control/optimize the spreading matrix  $\mathbf{S}$  for the G-MAC, while the MIMO channel coefficient matrix  $\mathbf{H}$  depends wholly on the fading channel realization which cannot be controlled. In addition, the conversion from a  $K$ -by- $N$  complex-valued model to a  $2K$ -by- $2N$  real-value model in (3) enables us to directly utilize the (real-value based) LCMA algorithms developed above.

#### V. ON THE OPTIMIZED DESIGN OF LCMA

##### A. Design of ILC Coefficient Matrix $\mathbf{A}$

In this section, we focus on LCMA with linear detection and provide a efficient yet powerful pragmatic solution to<sup>8</sup>  $\mathbf{A}$ , for a given spreading matrix  $\mathbf{S}$ . Following the convention in studying uplink MA, we consider that all users have symmetric rate. Our development can be extended to non-symmetric rates. For a given spreading matrix  $\mathbf{S}$ , let the minimum mean square error (MMSE) matrix be denoted by  $\Psi = (\rho \mathbf{S}^T \mathbf{S} + \mathbf{I}_K)^{-1}$ . Its eigen-decomposition is

$$\Psi = \mathbf{V} \mathbf{D} \mathbf{V}^T. \quad (36)$$

The rate for reliable communication of LCMA is characterized in the following theorem.

*Theorem 1:* A symmetric rate  $R_0$  is achievable if there exists  $K$  integer vectors  $\mathbf{a}_1, \dots, \mathbf{a}_K$ , that are linearly independent in  $\mathbb{Z}_{2^m}$ , such that

$$\mathbf{D}^{\frac{1}{2}} \mathbf{V}^T \mathbf{a}_l < \sqrt{\frac{1}{2^{2R_0}}}, \forall l = 1, \dots, K. \quad (37)$$

**Proof.** [Proof of Theorem 1] : It can be shown that the MSE in the linear estimator of  $\mathbf{a}_l^T \mathbf{x}[t]$  is  $\min_{\mathbf{w}_l} E(|\mathbf{w}_l^T \mathbf{y}[t] - \mathbf{a}_l^T \mathbf{x}[t]|^2)$

$$= \mathbf{a}_l^T (\rho \mathbf{S}^T \mathbf{S} + \mathbf{I}_K)^{-1} \mathbf{a}_l = \mathbf{a}_l^T \mathbf{V} \mathbf{D} \mathbf{V}^T \mathbf{a}_l. \quad (38)$$

As  $n$  tends to infinity, the effective noise sphere is given by this MSE value for computing the  $l$ th ILC. There exist a

<sup>8</sup>The optimized  $\mathbf{A}$  here is not optimal for the non-linear soft detectors [39], but also works reasonably well therein.

nested lattice-code with simultaneous ‘‘Roger-goodness’’ and ‘‘Poltyrev-goodness’’, such that the rate

$$R_l^{comp} = \frac{1}{2} \log_2^+ \left( \frac{1}{\mathbf{a}_l^T \mathbf{V} \mathbf{D} \mathbf{V}_l^T \mathbf{a}} \right). \quad (39)$$

w.r.t. the  $l$ th ILC is achievable [19], [23]. The overall achievable symmetric rate is given by  $R_0 \leq R_{sym}$  with

$$R_{sym} = \min_{l=1, \dots, K} R_l^{comp} = \min_{l=1, \dots, K} \frac{1}{2} \log_2^+ \left( \frac{1}{\mathbf{a}_l^T \mathbf{V} \mathbf{D} \mathbf{V}_l^T \mathbf{a}} \right).$$

Then, all  $K$  ILCs can be reliably computed if

$$\min_{l=1, \dots, K} \frac{1}{2} \log_2^+ \left( \frac{1}{\mathbf{a}_l^T \mathbf{V} \mathbf{D} \mathbf{V}_l^T \mathbf{a}} \right) > R_0, \quad (40)$$

then all users’ messages can be recovered. As (40) is equivalent to (37), the proof is completed. ■

*Remark 2:* The above characterization is based on the existence of nested lattices that are simultaneously good for shaping and channel-coding. For lattice-based processing with the practical ring-coded PAM, the achievable mutual information that takes into account the  $2^m$ -PAM should be used for characterization. However, for the case with a large number of UEs and BS antennas, it is well-known that calculating the exact mutual information for  $2^m$ -PAM requires a multi-dimension integration. This makes finding the optimized  $\mathbf{A}$  intangible. To obtain a viable and pragmatic solution to  $\mathbf{A}$ , in this paper we resort to the succinct rate expression (39) in our treatment. Optimization over such characterization yields a competitive solution for our developed LCMA with ring-coded PAM, as we will see in the next section.

Given Theorem 1, the problem is now to find  $K$  linearly independent lattice points, formed by the basis  $\mathbf{D}^{\frac{1}{2}} \mathbf{V}^T$ , within the boundary of radius  $\sqrt{\frac{1}{2^{2R_0}}}$ . This is referred to as a *bounded independent vectors problem* (BIVP). Solving the BIVP is easier than solving the shortest independent vector problem (SIVP), as one only need  $K$  independent points within the radius  $\sqrt{\frac{1}{2^{2R_0}}}$  rather than the  $K$  shortest ones. The linear independence of  $\mathbf{a}_1, \dots, \mathbf{a}_K$  is w.r.t.  $\mathbb{Z}_{2^m}$ , which guarantees that  $\mathbf{A} = \text{mod}(\mathbf{A}, 2^m)$  has a unique inverse in  $\mathbb{Z}_{2^m}$ . For a relatively large  $K$  and  $m$ , the linear independence w.r.t.  $\mathbb{Z}_{2^m}$  is equivalent to that in  $\mathbb{Z}$  in probability.

The most well-known approach, that may be borrowed to address the SIVP problem, would be the Lenstra–Lenstra–Lovász (LLL) algorithm [40]. The basic idea of the LLL algorithm is that, for a given set of lattice basis vectors, one carries out integer linear combinations of them to obtain new shorter lattice vectors. This step exploits the mechanism of Gram-Schmidt orthogonalization, with the weights being integers. The resultant vectors are then re-arranged (exchanged) in an increasing order of length, and the next round of integer linear combinations of the vectors are performed. In particular, the size-reduce condition and the Lovász condition are employed to guide the integer linear combinations and the exchanges of the lattice vectors. It is shown that LLL algorithm has a complexity order that is polynomial in  $K$ . However, for a large  $K$ , the performance loss of LLL becomes dramatic. The literature of

lattice reduction is rich in computer science area. Other well-known approaches for the SVP and SIVP include LLL-boost [41], HKZ [27], BKZ and BKZ 2.0 and etc.

In fact, we are not indeed solving the SIVP, but just the BIVP. Owing to this, we now propose a *rank-constrained sphere decoding* (RC-SD) algorithm which solves the BIVP in (37). The goal is to find  $K$  coefficient vectors  $\mathbf{a}_1, \dots, \mathbf{a}_K$  that are 1) within the boundary of radius  $\sqrt{\frac{1}{2^{2R_0}}}$  and 2) has full-rank  $K$ . In RC-SD, we start with an initial radius that is smaller than  $\sqrt{\frac{1}{2^{2R_0}}}$  and apply a sphere decoding tree search. If the rank for the candidates within the boundary is smaller than  $K$ , the radius is added by a certain small step and continue the tree search, until the rank reaches  $K$ . Then, we pick those  $K$  linearly independent vectors with smallest norms. The pseudo code for this approach is given in Algorithm 2.

---

#### Algorithm 2 Rank-constrained Sphere Decoding for identifying $\mathbf{A}$

---

Step 1) Set the radius to  $r = \sqrt{\frac{1}{2^{2R_0}}} - \varepsilon$ . The initial value can be set empirically.

Step 2) Implement the Cholesky factorization on  $\mathbf{V} \mathbf{D} \mathbf{V}_l^T$ , and apply a tree-search method which finds all candidates  $\mathbf{a}$  that are within distance  $r$  to the origin.

Step 3) If the rank of the candidates in  $\mathbb{Z}_{2^m}$  is less than  $K$ . Increase the radius  $r$  by a certain (small) step and Go to Step 1). Otherwise, continue to Step 4).

Step 4) Arrange the candidates with an ascending order according to the lengths. Start with the first candidate, use a greedy method to find  $K$  coefficient vectors, until the rank in reaches  $K$ .

---

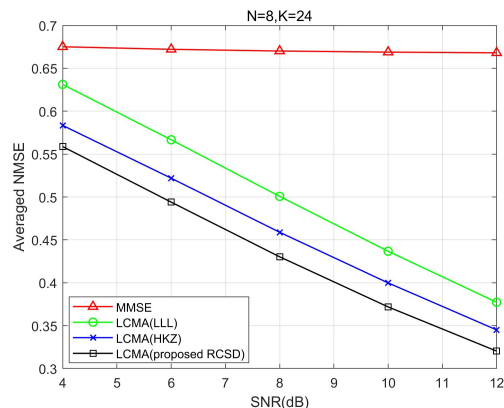


Fig. 2. Averages NMSE with the proposed RS-SD,  $N = 8, K = 24$ . The channel coefficients follows Rayleigh distribution.

Fig. 2 shows the averaged normalized MSE (NMSE) w.r.t. the ILCs where  $N = 8, K = 24$ , i.e., the system load of LCMA is 300%. Here  $\mathbf{S}$  is randomly given. It is well-known that NMSE characterizes the quality of the soft detection output. The smaller the NMSE, the greater the mutual information or supported code rate, following the notion of sphere-packing [42]. The conventional non-lattice-coded based scheme with MMSE detection fails to support this system load, as the MSE barely drops as SNR increases. In contrast, LCMA with any of the three methods for obtaining coefficient matrix  $\mathbf{A}$  can support a system load of 300%. In particular, our proposed RC-SD



method considerably outperforms existing LLL and HKZ lattice reduction methods [27]. We note that the efficiency of RC-SD algorithm may be further improved by jointly considering the full-rank condition in reducing the dimension of the search space, which will be investigated in future work.

Notably, LCMA is different from lattice-reduction based MIMO detection [27]. LCMA utilizes an  $n$ -dimension ring-coded PAM as the underlying coding-modulation, where the lattice is characterized by the generator matrix  $\mathbf{G}$ . The optimization of LCMA is based on the lattice obtained from the MMSE matrix. Lattice-reduction based MIMO detection is dealing with the lattice generated by the channel matrix  $\mathbf{H}$ . Our work differs from the lattice partition multiple access scheme [43] in the following. First, [43] considered a closed-loop downlink scenario and utilized superposition of the multiple users' signals via lattice partitioning. Only the theoretical rate was studied while no practical lattice codes were studied therein. In contrast, our work considers an open-loop uplink system, and is based on the property of the underlying lattice code (in the form of a practical 2-ary ring coded PAM). The dramatic improvement in terms of system load and BLER is presented. Second, the notions of structured binning and the computation of integer linear combinations, exploited in our work, are not relevant to the work in [43]. Furthermore, [43] was based on the successive cancellation procedures at the UE nodes, while in our work parallel processing procedures are utilized at the BSs. New algorithms for identifying the optimized  $\mathbf{A}$  matrix and the spreading matrix are developed in our work, which are not studied in [43].

### B. Design of LCMA Signature Sequences $\mathbf{S}$

So far we have presented the algorithms of the LCMA receiver: the soft ILC detection and the identification of  $\mathbf{A}$ . We are now in the position to study the spreading signature sequences  $\mathbf{S} = [\mathbf{s}_1, \dots, \mathbf{s}_K]$  for LCMA. Obviously, the performance of LCMA is a function of both  $\mathbf{S}$  and  $\mathbf{A}$ , and the joint optimized design problem is formulated as

$$\arg \max_{\mathbf{S}, \mathbf{A}} \min_l \frac{1}{2} \log_2^+ \left( \frac{1}{\mathbf{a}_l^T (\rho \mathbf{S}^T \mathbf{S} + \mathbf{I}_K)^{-1} \mathbf{a}_l} \right) \quad (41)$$

$$\text{s.t. } \text{Tr} \{ \mathbf{S}^T \mathbf{S} \} \leq K, \mathbf{A} \in \mathbb{Z}^{K \times K} \text{ has full rank } K,$$

where a total power constraint is considered. The formulation w.r.t. individual power constraint just needs to modified the power constraint into the form  $\|\mathbf{s}_i\|^2 \leq 1, \forall i = 1, \dots, K$ .

In this paper, we suggest a pragmatic method that decouples the optimization of  $\mathbf{S}$  and  $\mathbf{A}$  as follows. First, we solve the optimization of  $\mathbf{S}$  for a given  $\mathbf{A}$ . A local optima to the problem in (41) can be approximately found using a target-switching steepest descent (TS-SD) algorithm. The main idea of the TS-SD method is that the steepest descent based optimization process always targets on the ILC stream with the lowest compute rate, i.e.,

$$l_{min} = \arg \min_l R_l^{Comp} \quad (42)$$

where  $R_l^{Comp}$  is given in (39). For the  $l_{min}$ -th ILC, we establish a Lagrangian function as

$$\varphi(\mathbf{S}, u) = \mathbf{a}_{l_{min}}^T (\rho \mathbf{S}^T \mathbf{S} + \mathbf{I}_K)^{-1} \mathbf{a}_{l_{min}} + u(\text{tr}(\mathbf{S}^T \mathbf{S}) - K). \quad (43)$$

The steepest descent direction is obtained by taking the partial derivatives of  $\varphi(\mathbf{S}, u)$  w.r.t.  $\mathbf{S}$  and  $u$ , given by

$$\frac{\partial \varphi(\mathbf{S}, u)}{\partial \mathbf{S}} = 2u\mathbf{S} - 2\rho\mathbf{S}(\rho\mathbf{S}^T\mathbf{S} + \mathbf{I}_K)^{-1} \mathbf{a}_{l_{min}} \mathbf{a}_{l_{min}}^T (\rho\mathbf{S}^T\mathbf{S} + \mathbf{I}_K)^{-1}, \quad (44)$$

$$\frac{\partial \varphi(\mathbf{S}, u)}{\partial u} = \text{tr}(\mathbf{S}^T \mathbf{S}) - K. \quad (45)$$

Then,  $\mathbf{S}$  is updated by

$$\mathbf{S} = \mathbf{S} - \alpha(2u\mathbf{S} - 2\rho\mathbf{S}(\rho\mathbf{S}^T\mathbf{S} + \mathbf{I}_K)^{-1} \mathbf{a}_{l_{min}} \mathbf{a}_{l_{min}}^T (\rho\mathbf{S}^T\mathbf{S} + \mathbf{I}_K)^{-1}) \quad (46)$$

where  $\alpha$  is the update step (or learning rate). We consider that  $\alpha$  is a sampling value of a hyperbolic tangent function. Note that the initial value of  $u$  should be made larger than  $\alpha$  for the stability purpose of the iterative process. Also,  $u$  is updated by

$$u = u + \alpha(\text{tr}(\mathbf{S}^T \mathbf{S}) - K). \quad (47)$$

The update continues in an iterative manner as in standard SD. pseudo code for the SD step is presented in Algorithm 3.

Next, for the given  $\mathbf{S}$ , solve the optimization of  $\mathbf{A}$  as in (37) with the RC-SD algorithm. Then, carry out iterations between the above two steps until convergence is achieved.

As the optimization of spreading sequences  $\mathbf{S}$  is off-line, one may assign various initial values of  $\mathbf{S}$  (or  $\mathbf{A}$ ) and select the one with the best cost function to approximate the global optima.

---

#### Algorithm 3 Target-switching Steepest Descent

---

**Input:**  $N_S, K, \rho, \alpha, u^{(0)}$

**Output:**  $\mathbf{S}_{opt}$

Initialization:  $k = 0, \mathbf{S}^{(0)} = \text{randn}(N, K), \mathbf{S}^{(1)} =$

$\frac{\mathbf{S}}{\sqrt{\text{tr}(\mathbf{S}^T \mathbf{S})/K}}$

**while**  $\mathbf{S}^{(k+1)} \neq \mathbf{S}^{(k)}$  **do**

$k \leftarrow k + 1$

$l_{min} \leftarrow \min(R_1^{Comp}, \dots, R_K^{Comp})$

$\mathbf{S}^{(k+1)} \leftarrow \mathbf{S}^{(k)} - \alpha(2u^{(k)}\mathbf{S}^{(k)} - 2\rho\mathbf{S}^{(k)})$

$(\rho\mathbf{S}^{(k)T}\mathbf{S}^{(k)} + \mathbf{I}_K)^{-1} \mathbf{a}_{l_{min}} \mathbf{a}_{l_{min}}^T (\rho\mathbf{S}^{(k)T}\mathbf{S}^{(k)} + \mathbf{I}_K)^{-1}$

$u^{(k+1)} \leftarrow u^{(k)} + \alpha(\text{tr}(\mathbf{S}^{(k+1)T}\mathbf{S}^{(k+1)}) - K)$

**end while**

$\mathbf{S}_{opt} = \mathbf{S}^{(k)}$

---

Fig. 3 presents the achievable rate of LCMA in an Gaussian MA channel using our developed TS-SD method. Here we present with  $N_S = 8, K = 16, 24$ . For SNR greater than 4 dB, the difference between the achievable symmetric rate of LCMA and that of the upper bound (UB) of the MA channel capacity is almost unnoticeable for  $K=16$ , and is quite small (about 0.05 bit) for  $K=24$ . At low SNRs, the gap becomes greater. This is due to the well-known inherent loss of the lattice-code based scheme that achieves  $\frac{1}{2} \log^+(\varkappa + SNR)$ , with  $\varkappa < 1$  in general [19], [20]. We also include the performance with a long IRA code. For  $K = 16$ , at BER of  $10^{-4}$ , the performance is about 0.71 dB and 1.04 dB away from the rate limit of LCMA and MA capacity upper bound, respectively.

## VI. NUMERICAL RESULTS

### A. LCMA for Gaussian MA Channel

Fig. 3 also includes the performance of LCMA for Gaussian MA channel with a capacity approaching irregular repeat

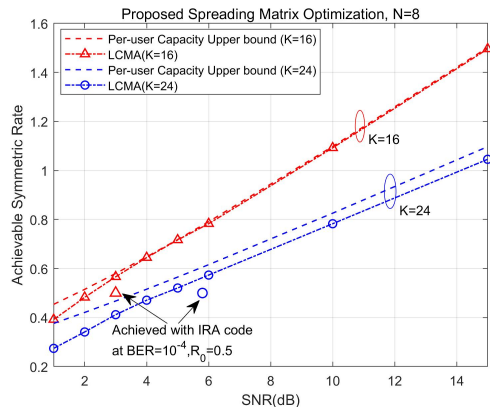


Fig. 3. Achievable symmetric rate per-user of LCMA with our designed spreading matrix  $\mathbf{S}$  in Gaussian MA channel, where  $N_S = 8$ ,  $K=16$  and 24. Total power constraint is utilized here. Note that the horizontal axis denotes the per-user SNR, while the vertical axis denotes the per-user rate. The sum-rate is equal to  $K$  times the per-user rate.

accumulate (IRA) code. The rate 1/2 binary irregular repeat accumulate (IRA) code of length  $k = 65536$  is from that in [5] optimized for single-user point-to-point AWGN channel. The utilization of a long IRA code is for the sake of comparison to the capacity limit. We observe that for  $K = 16$ , at BER of  $10^{-4}$ , the performance is about 0.71 dB and 1.04 dB away from the rate limit of LCMA and MA capacity UB, respectively. For  $K = 24$ , the performance is about 1.09 dB and 1.79 dB away from the rate and capacity limits. The performance behavior of LCMA with a practical IRA code is in line with the theoretical achievable rate result shown in Fig. 3.

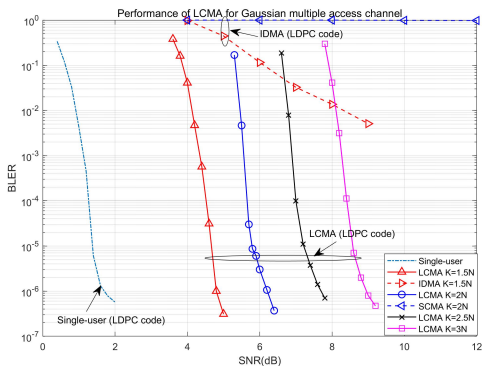


Fig. 4. BER of LCMA in Gaussian MA channel with  $N_S = 8$ . BPSK and a rate 1/2 LDPC code of length  $k = 3840$  are utilized. The individual power constraint is utilized in designing the spreading matrix  $\mathbf{S}$ .

Fig. 4 shows the BLER of LCMA with  $N_S = 8$  and  $K = 16, 20, 24$ , where a rate 1/2 length-3840 LDPC code in the 5G NR standard and BPSK are used. The spreading matrices used for system loads 150% and 200% are shown in Table I and II, respectively<sup>9</sup>. We also compare to existing non-lattice based IDMA system with chip-level interleaving and iterative elementary signal estimation (ESE) detection, and SCMA system with iterative message passing detection

<sup>9</sup>The spreading matrices for system loads 250% and 300% are too large to be presented here. Interested readers may contact us to request the spreading matrices for any system loads.

and decoding<sup>10</sup>. For a fair comparison, all MA schemes have identical power among  $K$  users. It is observed that LCMA

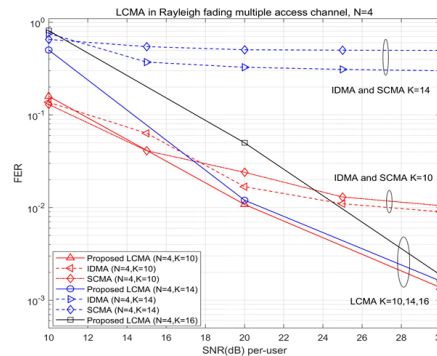


Fig. 5. BLER of LCMA with QPSK in fading MAC,  $N = 4$ .

exhibits the following advantages. First, LCMA supports all system loads under consideration. In contrast, IDMA and SCMA fail to support a system load greater than 200%. This is due to the poor adaptation of the 5G LDPC code with the ESE or message passing detector, i.e., a poor convergence behavior of the iterative detection and decoding (IDD) following the principle of EXIT chart. Due to the nature of parallel processing of LCMA, the convergence problem is not relevant, thus the stronger the underlying channel code is, the better the performance. We note that such competitive performance is achieved with merely parallel processing and  $K$  single-user decoding, without using successive cancellation or IDD. Second, excellent BLER performance of as low as  $10^{-6}$  to  $10^{-7}$  was demonstrated for LCMA, for all system loads under consideration. In practice, the very low BLER may help with ultra-reliable low-latency communication on top of massive access, by significantly reducing requests for MU-ARQ retransmission. Lastly, it is shown that, the supported system load by LCMA increase by 50% for every SNR increase of about 1.5 dB. Such consistent behavior was not reported for other existing MA schemes in the literature, to the best of our knowledge.

Fig. 5 shows the frame error performance in a fading MAC, where the spreading sequence developed for the Gaussian MAC is used. At the receiver side, the effective channel matrix is given by the combination of the spreading matrix  $\mathbf{S}$  and the complex-valued channel gain  $h_i, i = 1, \dots, K$ . It is demonstrated that LCMA can support up to  $K=16$  users with a spreading sequence length  $N = 4$ , which considerably outperforms existing IDMA and SCMA schemes.

### B. LCMA for MU-MIMO

Here we present the numerical results for MU-MIMO where the receiver is equipped with  $N_R$  antennas. The channel coefficients follow the Rayleigh distribution. In this setting, the iterative ESE or BP algorithms are implemented in the form of an iterative linear MMSE soft cancellation algorithm: the signal

<sup>10</sup>We do not include comparison to RSMA, as it is for the close-loop MA system where rate allocation is employed [13]. We do not include PDMA, MUSA and etc. for comparison, as their mechanisms are not largely different to IDMA and SCMA.

TABLE I  
EXAMPLE OF SPREADING SEQUENCE OF LCMA,  $K=12$ ,  $N_S=8$ .

-0.4150	0.4828	-0.0700	-0.4150	0.4828	-0.0700	-0.4150	0.4828	-0.0700	-0.4150	0.4828	-0.0700
-0.4150	0.4828	-0.0700	0.4150	-0.4828	0.0700	-0.4150	0.4828	-0.0700	0.4150	-0.4828	0.0700
-0.4150	0.4828	-0.0700	-0.4150	0.4828	-0.0700	0.4150	-0.4828	0.0700	0.4150	-0.4828	0.0700
-0.4150	0.4828	-0.0700	0.4150	-0.4828	0.0700	0.4150	-0.4828	0.0700	-0.4150	0.4828	-0.0700
0.2789	0.1300	0.4951	0.2789	0.1300	0.4951	0.2789	0.1300	0.4951	0.2789	0.1300	0.4951
0.2789	0.1300	0.4951	-0.2789	-0.1300	-0.4951	0.2789	0.1300	0.4951	-0.2789	-0.1300	-0.4951
0.2789	0.1300	0.4951	0.2789	0.1300	0.4951	0.1300	0.4951	-0.2789	-0.1300	-0.4951	0.2789
0.2789	0.1300	0.4951	-0.2789	-0.1300	-0.4951	-0.2789	-0.1300	-0.4951	0.2789	0.1300	0.4951

TABLE II  
EXAMPLE OF SPREADING SEQUENCE OF LCMA,  $K=16$ ,  $N_S=8$ .

0	0.2789	0.4850	0.4702	0	0.2789	0.4850	0.4702	0	0.2789	0.4850	0.4702	0	0.2789	0.4850	0.4702
0	0.2789	0.4850	0.4702	0	-0.2789	-0.4850	-0.4702	0	0.2789	0.4850	0.4702	0	-0.2789	-0.4850	-0.4702
0	0.2789	0.4850	0.4702	0	0.2789	0.4850	0.4702	0	-0.2789	-0.4850	-0.4702	0	-0.2789	-0.4850	-0.4702
0	0.2789	0.4850	0.4702	0	-0.2789	-0.4850	-0.4702	0	0.2789	0.4850	0.4702	0	0.2789	0.4850	0.4702
0.5000	0.4150	0.1216	-0.1700	0.5000	0.4150	0.1216	-0.1700	0.5000	0.4150	0.1216	-0.1700	0.5000	0.4150	0.1216	-0.1700
0.5000	0.4150	0.1216	-0.1700	-0.5000	-0.4150	-0.1216	0.1700	0.5000	0.4150	0.1216	-0.1700	-0.5000	-0.4150	-0.1216	0.1700
0.5000	0.4150	0.1216	-0.1700	0.5000	0.4150	0.1216	-0.1700	-0.5000	-0.4150	-0.1216	0.1700	-0.5000	-0.4150	-0.1216	0.1700
0.5000	0.4150	0.1216	-0.1700	-0.5000	-0.4150	-0.1216	0.1700	0.5000	0.4150	0.1216	-0.1700	-0.5000	-0.4150	-0.1216	0.1700

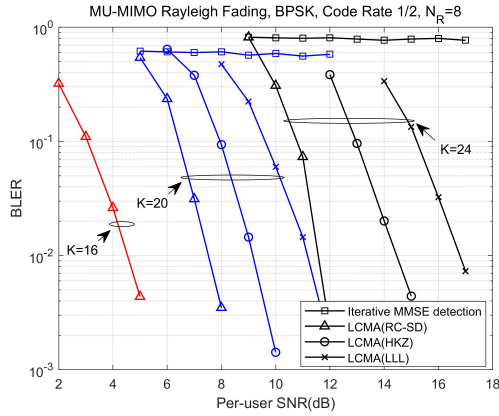


Fig. 6. BLER of LCMA in multi-user MIMO of  $N_R = 8$  receive antennas. LCMA can support a system load of no less than 300%, while the baseline scheme with iterative receiver cannot support a load greater than 200%.

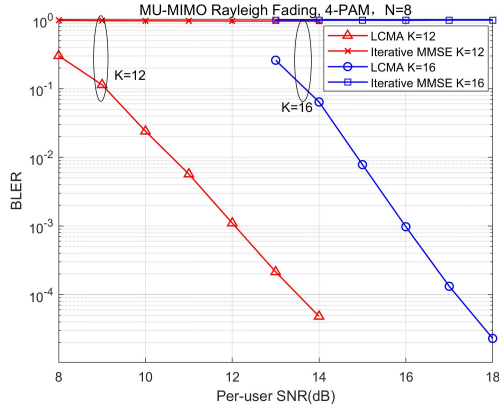


Fig. 7. BLER of LCMA with 4-PAM in MU-MIMO,  $N_R = 8$ ,  $K=12$  and 16. For 4-PAM, LCMA can support a system load of at least 200%, while iterative MMSE detection fails to converge.

of each received antenna can be viewed as a chip-level signal in IDMA/SCMA; the chip-level cancelation with elementary extrinsic information feedback is conducted; the linear MMSE filtering combines all  $N_R$  received antennas' signals.

Fig. 6 shows the BLER of LCMA where  $N_R = 8$  and  $K = 16, 20, 24$ . BPSK and a length-480 5G NR LDPC code

of rate  $k/m=1/2$  are utilized.  $Q = 10$  receiver iterations are implemented in iterative MMSE detection. Perfect receiver-side CSI is considered in the simulation. It is clear that LCMA can support a system load of no less than 300%, while the baseline scheme with iterative receiver cannot support a system load greater than 200% where the BLER curve flats out.

We next consider MA with higher level modulations, e.g.,  $2^m$ -PAM (or  $2^{2m}$ -QAM). Each user utilizes the  $2^m$ -ary ring code for encoding (4) and mapped to  $2^m$ -PAM. Fig. 7 shows the BLER of LCMA with  $m = 2$  (4-PAM), code rate  $k/n = 1/2$ ,  $N_R = 8$ ,  $K=12$  and 16. The information rate is 12 and 16 bits per channel-use per real dimension, respectively. The detail of the underlying ring code can be found in [37]. It is demonstrated that for 4-PAM, LCMA can support a system load of at least 200% with using only parallel processing. In contrast, iterative MMSE detection with 4-PAM fails to converge at this system load. We again note that a  $2^m$ -ary ring-code is required in LCMA for 4-PAM. Existing schemes such BICM and TCM are not lattice codes hence does not support the LCMA processing.

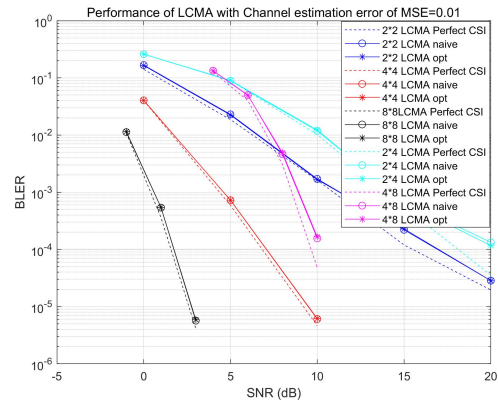


Fig. 8. BLER of LCMA with QPSK in MU-MIMO with imperfect CSI.

We note that any existing method for training sequence design and channel estimation algorithm for  $\mathbf{H}$  can be adopted, such as the minimum mean square error (MMSE) and approximate message passing (AMP) methods. No extra requirement of channel estimation is needed for implement LCMA. Fig. 8 shows the numerical results of LCMA with imperfect channel estimation where the MSE of channel estimation is 0.01. It is

observed that as the dimension of the MA system increases, the loss due to channel estimation error becomes insignificant.

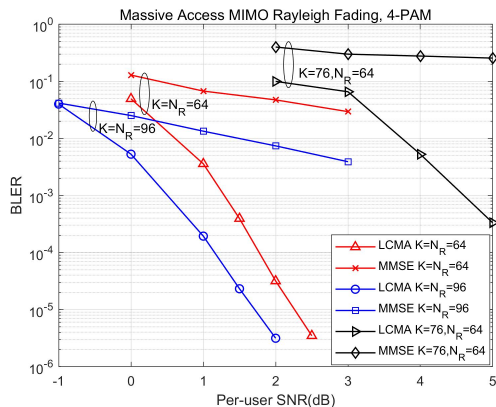


Fig. 9. BLER of LCMA in massive-access MIMO of  $N_R = 64$  and 96 and receive antennas, where 4-PAM and the rate half 4-ary ring code is used. LCMA vastly outperforms conventional MMSE receiver.

### C. LCMA for Massive-Access MIMO

Fig. 9 presents the numerical results for the massive-access MIMO setup where the receiver is equipped with a large number of antennas, i.e.  $N_R=64$  and 96, while the number of UEs  $K$  is no smaller than  $N_R$ . In this setting, we compare to linear MMSE receiver. It is observed that LCMA vastly outperforms the conventional baseline scheme for the massive-access MIMO setup. LCMA can achieve a BLER as low as  $10^{-6}$ , which is far beyond the capability of the conventional scheme. For the setup with  $K = 76$ ,  $N_R = 64$ , the BLER of the baseline scheme flats out while LCMA reaches  $3 \times 10^{-4}$  at 5 dB.

### D. Analysis of Implementation Costs of LCMA

The orders of complexities are shown in Table. III. The typical value of receiver iterations  $Q$  is between 4 to 10 for IDMA/SCMA. The computation in LCMA consists of 1) channel-code decoding, 2) LCMA soft detection, and 3) identification of  $\mathbf{A}$ . For 1), LCMA requires only  $K$  decoding operations while IDMA/SCMA requires  $Q$  times more. For the uplink MA, the modulation order  $q = 2^m$  is usually not large, where the complexity of ring-code decoding is not considerably greater than that based on binary channel code decoding.

For 2), LCMA needs to compute  $K$  streams of APPs w.r.t. the ILCs, while IDMA/SCMA requires to compute  $Q \cdot K$  streams of soft estimates. In particular, if Detection methods II or III is utilized, the per-symbol detection complexity (of calculating the distance and the likelihood function) of stream  $l$  is of order  $O((q-1)\omega_H(\mathbf{a}_l))$ , where  $\omega_H(\mathbf{a}_l) < K$  denotes the weight of the coefficient vector  $\mathbf{a}_l$ . The average detection complexity of LCMA is thus  $O(Kn(q-1)E(\omega_H(\mathbf{a})))$ . In contrast, the iterative chip-by-chip detection of IDMA has a complexity of  $O(Q \cdot Kn \log_2^q N_S)$ , while that of SCMA is  $O(Q \cdot Kn \log_2^q E(\omega(\mathbf{s})))$  where  $E(\omega(\mathbf{s}))$  denotes the average number of non-zero entries of the spreading sequence  $\mathbf{s}$ . Due to the avoidance of iterative detection, the overall detection complexity of LCMA is smaller than that of IDMA/SCMA.

For 3), with LLL, the complexity is between  $O(K^3)$  and  $O(K^4)$ , a polynomial in  $K$ . The complexity of HKZ and RC-SD is moderately higher than LLL. Since  $\mathbf{A}$  is chosen once per block, for a moderate-to-long block length  $n$  (e.g.  $n > 480$ ), this overhead is not significant. We next discuss

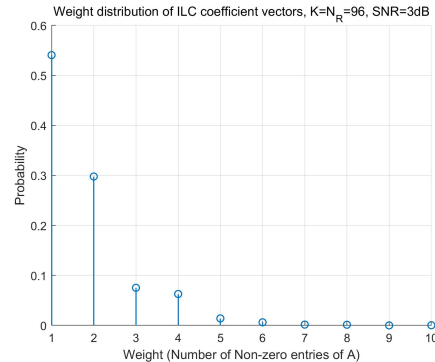


Fig. 10. Weight distribution of the ILC coefficient vector for massive-access MIMO of  $K = N_R = 96$ .

the complexity of LCMA for massive-access MIMO. Fig. 10 shows the distribution of the number of non-zeros entries (i.e. the weight) of the ILC coefficient vectors  $\mathbf{a}$ . This figure means that, although the number of UEs  $K$  is quite large,  $\mathbf{A}$  is a reasonably sparse matrix, i.e. more than 90% ILC coefficient vectors are of weights less than 5. Recall from Section IV that the average per-user complexity has order  $O(2^m E_{\mathbf{a}}(\omega_H(\mathbf{a})))$ . This is  $E(\omega_H(\mathbf{a}))$  times of the complexity of single-user detection. Fig. 10 shows that  $E_{\mathbf{a}}(\omega_H(\mathbf{a}))$  is just a very small fraction of  $K$  in general. As such, LCMA has a very low complexity for massive access MIMO.

There are other features that may be desired for implementation. First, note that the  $Q$  consecutive receiver iterations in IDMA/SCMA are executed in serial. Since IDD is avoided, LCMA with parallel processing incurs a much smaller latency. Second, there is no need to store the chip-level soft extrinsic information updated in IDD, which may reduce the memory occupation. Last but not that least, for BPSK/QPSK, off-the-shelf channel codes in various standards can be directly used in LCMA, regardless of the system load  $\frac{K}{N}$ . In contrast, as the load  $\frac{K}{N}$  varies, IDMA and SCMA have to adopt different codes. Otherwise, the convergence of IDD may not be achieved, leading to impaired performance or even failed functionality.

## VII. CONCLUSIONS

We presented a LCMA scheme and a package of algorithms that are essential to its implementation, including the  $2^m$ -ary ring-coded PAM, LCMA soft detection algorithms, rate-constrained sphere-decoding for solving the BIVP that identifies the optimized coefficient matrix  $\mathbf{A}$ , and a pragmatic solution for optimizing the MA spreading matrix  $\mathbf{S}$ . The per-user detection complexity is of order less than  $O(K)$ , suitable for massive access. With just parallel processing, considerable system load and error rate performance enhancement were demonstrated, without using successive interference cancellation or iterative detection. Off-the-shelf binary codes such as 5G NR LDPC codes can be directly used in LCMA for any system load,

TABLE III  
THE ORDERS OF COMPLEXITIES OF LCMA, IDMA AND SCMA SYSTEMS

	Detection	Decoding	Coefficient Identification	Interleaver&De-interleaver
LCMA	$O(Knq \cdot E(\omega_H(\mathbf{a})))$ for Det. Method II and III, $O(Kn \mathcal{L} )$ for Method I	$O(Kn(q-1))$	Between $O(K^3)$ and $O(K^4)$	not required
IDMA	$O(Q \cdot Kn \log_2^q \cdot N_S)$	$O(Q \cdot Kn \log_2^q)$	not required	$O(2Q \cdot Kn \cdot N_S)$
SCMA	$O(Q \cdot K^2 n \log_2^3)$	$O(Q \cdot Kn \log_2^q)$	not required	$O(2Q \cdot Kn)$

avoiding the issue of adaptation of channel-code and multi-user detector. Excellent BLER performance of as low as  $10^{-6}$  to  $10^{-7}$  was demonstrated for LCMA, for all system loads under consideration. Such very low BLER may help with ultra-reliable low-latency communication on top of massive access, by tremendously slashing request of MU-ARQ retransmission.

## REFERENCES

- [1] W. Tong and P. Zhu, "6G the next horizon-from connected people and things to connected intelligence," *Cambridge University Press*, 2021.
- [2] L. Dai, B. Wang, Z. Ding, Z. Wang, S. Chen, and L. Hanzo, "A survey of non-orthogonal multiple access for 5G," *IEEE Communications Surveys and Tutorials*, vol. 20, no. 3, pp. 2294–2323, 2018.
- [3] Z. Ding, Y. Liu, J. Choi, Q. Sun, M. Elkashlan, I. Chih-Lin, and H. V. Poor, "Application of non-orthogonal multiple access in LTE and 5G networks," *IEEE Commun. Mag.*, vol. 55, no. 2, pp. 185–191, 2017.
- [4] T. M. Cover and J. A. Thomas, "Elements of information theory," *John Wiley & Sons, Inc.*, 1991.
- [5] S. ten Brink and G. Kramer, "Design of repeat-accumulate codes for iterative detection and decoding," *IEEE Trans. Signal Processing*, vol. 51, no. 11, pp. 2764–2772, 2003.
- [6] S. R. Islam, N. Avazov, O. A. Dobre, and K.-S. Kwak, "Power-domain non-orthogonal multiple access (NOMA) in 5G systems: Potentials and challenges," *IEEE Commun. Surv. Tuts.*, vol. 19, no. 2, pp. 721–742, 2016.
- [7] X. Wang and H. V. Poor, "Iterative (turbo) soft interference cancellation and decoding for coded CDMA," *IEEE Trans. Comm.*, vol. 47, no. 7, pp. 1046–1061, 1999.
- [8] P. Li, L. Liu, K. Wu, and W. Leung, "Interleave division multiple-access," *IEEE Trans. Wireless Comm.*, vol. 5, no. 4, pp. 938–947, Apr. 2006.
- [9] H. Nikopour and H. Baligh, "Sparse code multiple access," in *Proc. IEEE 24th Int. Symp. Pers. Indoor Mobile Radio Commun. (PIMRC)*, pp. 332–336, 2013.
- [10] S. Kudekar and K. Kasai, "Spatially coupled codes over the multiple access channel," in *2011 IEEE International Symposium on Information Theory Proceedings*, pp. 2816–2820, 2011.
- [11] T. Yang, J. Yuan, and Z. Shi, "Rate optimization for IDMA systems with iterative joint multi-user decoding," *IEEE Trans. Wireless Comm.*, vol. 8, no. 3, pp. 1148–1153, Mar. 2009.
- [12] B. Rimoldi and R. Urbanke, "A rate-splitting approach to the Gaussian multiple-access channel," *IEEE Transactions on Inf. Theory*, vol. 42, no. 2, pp. 364–375, 1996.
- [13] Y. Mao, B. Clerckx, and V. O. K. Li, "Rate-splitting for multi-antenna non-orthogonal unicast and multicast transmission: Spectral and energy efficiency analysis," *IEEE Trans. Comm.*, vol. 67, no. 12, pp. 8754–8770, 2019.
- [14] S. Chen, B. Ren, Q. Gao, S. Kang, S. Sun, and K. Niu, "Pattern division multiple access—A novel nonorthogonal multiple access for fifth-generation radio networks," *IEEE Trans. Vehi. Tech.*, vol. 66, no. 4, pp. 3185–3196, 2016.
- [15] Y. Cheng, L. Liu, and L. Ping, "Orthogonal AMP for massive access in channels with spatial and temporal correlations," *IEEE J. Sel. Areas Commun.*, vol. 39, no. 3, pp. 726–740, 2021.
- [16] Z. Sun, Y. Xie, J. Yuan, and T. Yang, "Coded slotted aloha for erasure channels: Design and throughput analysis," *IEEE Trans. Commun.*, vol. 65, no. 11, pp. 4817–4830, 2017.
- [17] E. Paolini, G. Liva, and M. Chiani, "Coded slotted aloha: A graph-based method for uncoordinated multiple access," *IEEE Trans. Inf. Theory*, vol. 61, no. 12, pp. 6815–6832, 2015.
- [18] R. Zamir, S. Shamai, and U. Erez, "Nested linear/lattice codes for structured multiterminal binning," *IEEE Trans. Inf. Theory*, vol. 48, no. 6, pp. 1250–1276, 2002.
- [19] B. Nazer and M. Gastpar, "Compute-and-forward: Harnessing interference through structured codes," *IEEE Trans. Inf. Theory*, vol. 57, no. 10, pp. 6463–6486, Oct. 2011.
- [20] W. Nam, S. Chung, and Y. H. Lee, "Capacity of the Gaussian two-way relay channel to within 1/2 bit," *IEEE Trans. Inf. Theory*, vol. 56, no. 11, pp. 5488–5494, Nov. 2010.
- [21] X. Yuan, T. Yang, and I. Collings, "Multiple-input multiple-output two-way relaying: a space-division approach," *IEEE Trans. Inf. Theory*, vol. 59, no. 10, pp. 6421–6440, Oct. 2013.
- [22] S. H. Lim, C. Feng, A. Pastore, B. Nazer, and M. Gastpar, "Compute-forward for DMCs: Simultaneous decoding of multiple combinations," *IEEE Trans. Inf. Theory*, vol. 66, no. 10, pp. 6242–6255, 2020.
- [23] J. Zhan, B. Nazer, U. Erez, and M. Gastpar, "Integer-forcing linear receivers," *IEEE Trans. Inf. Theory*, vol. 60, no. 12, pp. 7661–7685, Dec. 2014.
- [24] D. Silva, G. Pivaro, G. Fraidenraich, and B. Aazhang, "On integer-forcing precoding for the Gaussian MIMO broadcast channel," *IEEE Trans. Wireless Comm.*, vol. 16, no. 7, pp. 4476–4488, 2017.
- [25] S.-N. Hong and G. Caire, "Compute-and-forward strategies for cooperative distributed antenna systems," *IEEE Trans. Inf. Theory*, vol. 59, no. 9, pp. 5227–5243, Sep. 2013.
- [26] T. Yang, "Distributed MIMO broadcasting: Reverse compute-and-forward and signal-space alignment," *IEEE Trans. Wireless Comm.*, vol. 16, no. 1, pp. 581–593, 2017.
- [27] A. Sakzad, J. Harshan, and E. Viterbo, "Integer-forcing MIMO linear receivers based on lattice reduction," *IEEE Trans. Wireless Comm.*, vol. 12, no. 10, pp. 4905–4915, 2013.
- [28] D. Yang and K. Yang, "Multimode integer-forcing receivers for block fading channels," *IEEE Transactions on Wireless Communications*, vol. 19, no. 12, pp. 8261–8271, 2020.
- [29] S. Lyu, A. Campello, and C. Ling, "Ring compute-and-forward over block-fading channels," *IEEE Transactions on Information Theory*, vol. 65, no. 11, pp. 6931–6949, 2019.
- [30] O. Ordentlich and U. Erez, "Cyclic-coded integer-forcing equalization," *IEEE Transactions on Information Theory*, vol. 58, no. 9, pp. 5804–5815, 2012.
- [31] J. Zhu and M. Gastpar, "Gaussian multiple access via compute-and-forward," *IEEE Trans. Inf. Theory*, vol. 63, no. 5, pp. 2678–2695, 2016.
- [32] E. Sula, J. Zhu, A. Pastore, S. H. Lim, and M. Gastpar, "Compute-forward multiple access (CFMA): Practical implementations," *IEEE Trans. Comm.*, vol. 67, no. 2, pp. 1133–1147, 2018.
- [33] Q. Chen, F. Yu, T. Yang, J. Zhu, and R. Liu, "A linear physical-layer network coding based multiple access approach," in *2022 IEEE International Symposium on Information Theory (ISIT)*, pp. 2803–2808, 2022.
- [34] Q. Chen, F. Yu, T. Yang, and R. Liu, "Gaussian and fading multiple access using linear physical-layer network coding," *IEEE Trans. Wireless Comm.*, early access, 2022.
- [35] T. Yang, L. Yang, Y. J. Guo, and J. Yuan, "A non-orthogonal multiple-access scheme using reliable physical-layer network coding and cascade-computation decoding," *IEEE Trans. Wireless Comm.*, vol. 16, no. 3, pp. 1633–1645, 2017.
- [36] U. Erez and S. ten Brink, "A close-to-capacity dirty paper coding scheme," *IEEE Trans. Inf. Theory*, vol. 51, no. 10, pp. 3417–3432, 2005.
- [37] F. Yu, T. Yang, and Q. Chen, "Doubly irregular repeat modulation codes over integer rings for multi-user communications," *ChinaComm.*, 2022, accepted.
- [38] L. Ping, L. Liu, K. Wu, and W. K. Leung, "Interleave division multiple-access," *IEEE Trans. Wireless Commun.*, vol. 5, no. 4, pp. 938–947, 2006.
- [39] T. Yang, "Beyond integer-forcing receiver for lattice-code based multi-user MIMO system," *IEEE Communications Letters*, vol. 27, no. 10, pp. 2553–2557, 2023.
- [40] H. W. J. L. L. Lenstra, A. K.; Lenstra, "Factoring polynomials with rational coefficients," *Mathematische Annalen*, vol. 261, no. 4, pp. 515–534, 1982.
- [41] S. Lyu and C. Ling, "Boosted KZ and LLL algorithms," *IEEE Transactions on Signal Processing*, vol. 65, no. 18, pp. 4784–4796, 2017.
- [42] U. Erez and R. Zamir, "Achieving  $\log(1+\text{SNR})$  on the AWGN channel with lattice encoding and decoding," *IEEE Trans. Inf. Theory*, vol. 50, no. 10, pp. 2293–2314, 2004.
- [43] D. Fang, Y.-C. Huang, Z. Ding, G. Geraci, S.-L. Shieh, and H. Claussen, "Lattice partition multiple access: A new method of downlink non-orthogonal multiuser transmissions," in *2016 IEEE Global Communications Conference (GLOBECOM)*, pp. 1–6, 2016.